Non-local effects of edge excitations in the quantum Hall regime

E.V. Deviatov,[1,*] A. Lorke,[2] G. Biasiol,[3] and L. Sorba[4]

[1] *Institute of Solid State Physics RAS, Chernogolovka, Moscow District, 142432, Russia*
[2] *Laboratorium für Festkörperphysik, Universität Duisburg-Essen, Lotharstr. 1, D-47048, Duisburg, Germany*
[3] *Laboratorio Nazionale TASC INFM-CNR, AREA Science Park, I-34012 Trieste, Italy*
[4] *NEST INFM-CNR and Scuola Normale Superiore, I-56126 Pisa, Italy*

(Dated: May 31, 2019)

We use a novel sample geometry to study non-local effects of edge excitations in the integer quantum Hall effect regime. We find that the condition of local equilibrium at the quantum Hall edge is affected by the diffusion of dynamically polarized nuclei. Our analysis indicates, that the nuclear diffusion is effectively one-dimensional in the present experiment.

PACS numbers: 73.40.Qv 71.30.+h

The importance of edge states (ES) was appreciated since the beginning of the quantum Hall (QH) investigations[1]. ES are arising near the sample edge at the intersections of the Fermi level and filled Landau levels. Transport through imbalanced ES allows to describe[2] different transport characteristics of the QH systems[3].

Even at low imbalances, transport between spin-split ES is a challenging scientific problem, because of an electron's spin flip necessity[4]. It was demonstrated, that transport between spin-split ES can partially go through the flip-flop process[5–7]. In this process, an electron spin-flip causes the spin-flop of a nucleus in the GaAs lattice as described by the hyperfine interaction Hamiltonian

$$A\boldsymbol{I}\cdot\boldsymbol{S} = \frac{1}{2}(I^+S^- + I^-S^+) + AS_zI_z,$$

where $A > 0$ is the hyperfine constant, $\boldsymbol{I}$ is the nuclear spin and $\boldsymbol{S}$ is the electron spin. As a result, a region of dynamically polarized nuclei (DNP) is created at the sample edge. The influence of the nuclear polarization $\langle I_z\rangle$ on the electron energy can be conveniently described by the effective Overhauser field.

Recently, a method was proposed[8] to create ES imbalances, exceeding the spectral gaps at the edge. Electron transport at high imbalances accompanies by exciting non-equilibrium electrons[8] and dynamically polarized nuclei in the integer QH regime[9]. Despite the different nature, these excitations are long-life enough to spread out far from the creation region. There, in turn, they may affect the electron transport between ES.

Here, we use a novel sample geometry to study non-local effects of edge excitations in the integer quantum Hall effect regime. We find that the condition of local equilibrium at the quantum Hall edge is affected by the diffusion of dynamically polarized nuclei. Our analysis indicates, that the nuclear diffusion is effectively one-dimensional in the present experiment.

Our samples are fabricated from a molecular beam epitaxially-grown GaAs/AlGaAs heterostructure. It contains a two-dimensional electron gas (2DEG) located 200 nm below the surface. The 2DEG mobility at 4K is $5.5\cdot10^6\mathrm{cm}^2/\mathrm{Vs}$ and the carrier density is $1.63\cdot10^{11}\mathrm{cm}^{-2}$.

Samples are patterned in a modified quasi-Corbino sample geometry, see Fig. 1, (a). Each sample has two macroscopic ($\sim 0.5\times0.5\mathrm{mm}^2$) etched regions inside, separated by 300 μm distance. Ohmic contacts are placed at the mesa edges. A split-gate, encircling the etched regions, is used to connect inner and outer mesa edges in a controllable way. Two 5 μm wide gate-gap regions at the outer mesa edge are separated by 30 μm gated region.

In real samples, each Landau level is pinned to the Fermi level in a finite region (compressible strip) instead of one-dimensional crossing, because of the smooth edge potential[10]. Below, we refer the compressible strips as the edge states (ES) for the sake of the simplicity, in the spirit of the initial definition[1,2]. They are at the electrochemical potentials of the corresponding Ohmic contacts. There are gaps at the Fermi level (incompressible strips) in between ES, see Fig. 1, (b). Each incompressible strip can be characterized by a constant local filling factor ν_c, which is smaller than the bulk filling factor ν.

We deplete the 2DEG to a lower integer or fractional filling factor $g < \nu$ under the gate. Only strips with $\nu_c < g$ are allowed at the gate-covered mesa edges, so the incompressible strip with $\nu_c = g$ separates ES in the gate-gap, originating from the inner and outer mesa edges. By applying a bias between the outer and inner contacts, we directly apply it between two ES in the gate-gap, separated by the incompressible strip with $\nu_c = g$.

In the case of transport between two spin-split ES (i.e. across the $\nu_c = g = 1$ incompressible strip), an electron spin is changed by spin-orbit coupling[4] or in the flip-flop process. The latter creates DNP in the gate-gap region[9], as described above. DNP spread out from the gate-gap region because of nuclear spin diffusion[11,12]. If the applied imbalance achieves the energy gap value in the $\nu_c = 1$ incompressible strip, the flat-band situation[8] is realized, see Fig 1, (c). In this case, electrons are injected to the empty (excited) energy level at the outer sample edge, see Fig 1, (c). They are leaving the gate-gap region at this non-equilibrium state, relaxing elsewhere vertically.

In the present experiment, we use transport in one gate-gap (the injector) to create DNP and non-equilibrium electrons, while another gate-gap region

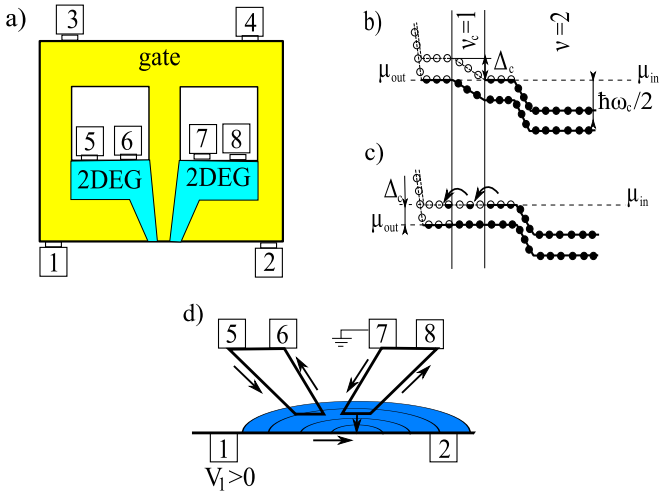

FIG. 1: (Color online) (a) Schematic diagram of the sample (not in the scale). The etched mesa edges are shown by thick solid lines. Light yellow (light gray) areas indicate the split-gate, that covers 2DEG around the inner etched regions and forms two 5 μm width gate-gap regions at the outer mesa edge, separated by the 30 μm distance. Light green (gray) area indicates uncovered 2DEG. Ohmic contacts are denoted by bars with numbers. (b,c) Schematic diagram of the energy levels in the gate-gap regions at integer filling factors $\nu = 2, g = 1$. Filled circles represent the fully occupied electron states in the incompressible strip and in the bulk. Half-filled circles indicate the partially occupied electron states in the compressible strips. Open circles are for the empty states. Δ_c is the potential jump in the ν_c incompressible strip. Pinning of the Landau sublevels to the Fermi level (shot-dash) is shown in the compressible regions at electrochemical potentials μ_{out} and μ_{in}. (b) Equilibrium situation $\mu_{out} = \mu_{in}$, no electrochemical imbalance is applied across the incompressible strip. (c) Flat-band conditions for the electrochemical potential imbalance $\mu_{in} - \mu_{out} = \Delta_c$. Arrows indicate a new way for electrons along the energy level. (d) Schematic diagram of the experiment (contact combination 1, see the text). Edge states in the active sample area are shown by bold lines. Ohmic contacts are denoted by bars with numbers. Arrows indicate a electrons' drift direction along ES and transport between two ES in the right (injector) gate-gap. The diffusion of the DNP from the injector region is shown by blue color.

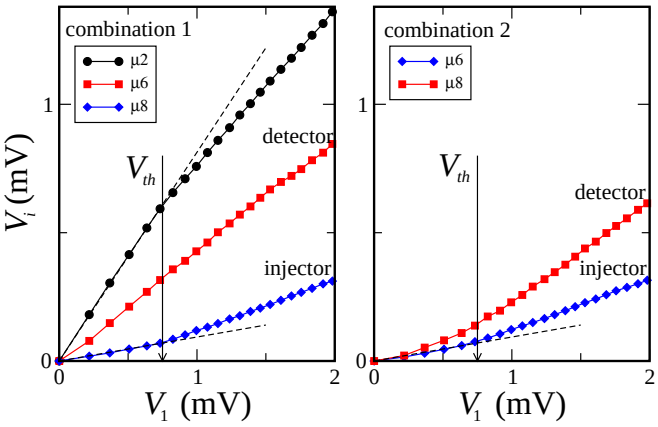

FIG. 2: (Color online) Potentials V_i of different Ohmic contacts ($eV_i = \mu_i, e < 0$) vs. applied potential V_1 for two contact combinations for the filling factors $\nu = 2, g = 1$. Potentials of the inner contacts in the injector region are depicted by blue line with diamonds. Ones for the detector region are shown by red line with squares. Left panel (combination 1): potentials of the contacts 2 (circles), 6 (squares), and 8 (diamonds). Right panel (combination 2): potentials of the contacts 6 (squares), and 8 (diamonds). Dash indicates slopes of the initial parts ($V_1 < V_{th} = 0.75$ mV) of the curves. Magnetic field equals to 3.68 T.

serves as a detector, see Figs. 1, (a,d). Contacts 2,6,8 are used to trace the electrochemical potentials of the corresponding ES. DC bias is always applied to the outer contact labeled as 1. The ground varies for two contact combinations:

(i) Contact combination 1. Contact 7 is grounded. The electrochemical potential imbalance is applied in the right gate-gap region in Fig 1, (d). It is used as an injector, the left one serves as a detector.

(ii) Contact combination 2. Contact 5 is grounded. The left gate-gap region is used as an injector, the right one serves as a detector.

These two contact combinations are not equivalent because of the chirality in the magnetic field. In our setup, electrons are moving counter-clockwise at the outer sample edge in Fig 1, (a,d). A high distance between gate-gap regions (30 μm) prevents a direct crosstalk.

The results presented below are independent of the cooling cycle. They are obtained in a dilution refrigerator at the base temperature of 30 mK. Standard two-point magnetoresistance is used to obtain the electron concentration in the ungated area and to verify the contact quality. Magnetocapacitance measurements are used to determine the available integer and fractional filling factors g under the gate.

The experimental results are shown in Fig. 2 for integer filling factors $\nu = 2, g = 1$ for two contact combinations. Voltage imbalance is applied between ES in the injector gate-gap region, because of the grounded contact inside it. In contrast, ES are expected to be in a local equilibrium in the detector gate-gap.

The potential of the inner contact in the injector region (μ_8^{comb1} or μ_6^{comb2} in the combinations 1 or 2, respectively) reflects transport between two ES, see Fig. 2. Each curve consists of two linear parts, so the slope is increased at some voltage $V_1 = V_{th}$. The change of the slope demonstrates the increase of the transport at high imbalances, i.e. $V_1 = V_{th}$ corresponds to the flat-band situation, see Fig 1, (c). We find $\mu_8^{comb1} = \mu_6^{comb2}$ at any applied imbalance, which indicates that both gate-gap regions are equivalent in the geometrical dimensions and 2DEG parameters.

The potential of the outer contact 2 in the combination 1 μ_2^{comb1} reflects the electrochemical potential of the outer compressible strip after leaving the injector region.

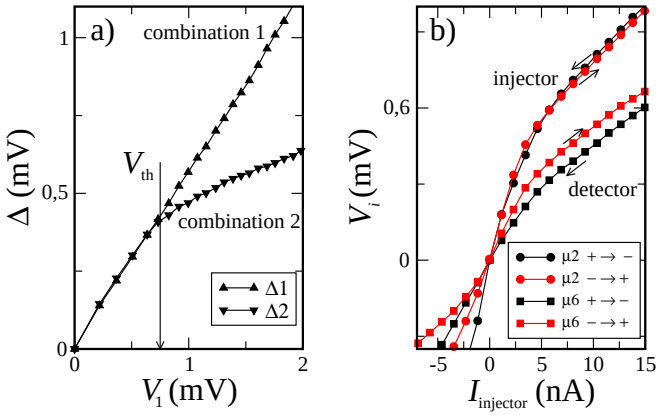

FIG. 3: (Color online) (a) Difference Δ between the expected and the measured signals (see Fig. 2 and the main text) for two contact combinations. (b) Potentials V_i of the contacts 2 (circles) and 6 (squares) as functions of the current $I_{injector}$ in the injector region for the two sweep directions. Contact combination 1, i.e. contact 7 is grounded. The curves are non-linear now, because the $I_{injector}$ is the non-linear function of V_1. Filling factors are $\nu = 2, g = 1$. Magnetic field equals to 3.68 T.

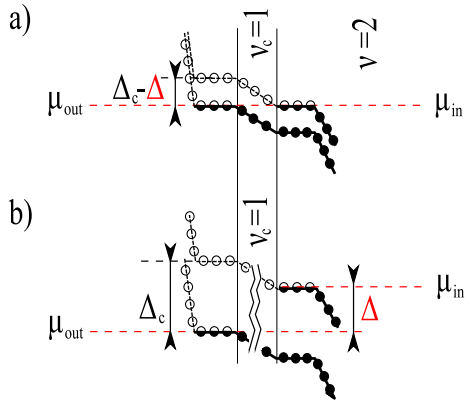

FIG. 4: (Color online) (a) Schematic diagram of the energy levels in the detector gate-gap regions at integer filling factors $\nu = 2, g = 1$. Local equilibrium is depicted $\mu_{out} = \mu_{in}$ within the DNP region. Zeeman splitting between ES Δ_c is diminished by the Overhauser shift Δ (typed in red). (b) ES leaving the DNP region. Disappearance of the Overhauser shift leads to the chemical potential imbalance $\mu_{in} - \mu_{out} = \Delta$ between ES. Note that ES are spatially separated in this case, so there is no transport between them.

The curve also consists of two linear parts, but the slope becomes *smaller* at V_{th}, see Fig. 2. This is completely consistent with the μ_8^{comb1} behavior, demonstrating increased transport above V_{th}. The slopes of both curves can be easily calculated[2,8]. The calculation gives exactly the same slopes as we see in the experiment, indicating that current is flowing in the injector region only. This excludes any parasitic ground within the detector region.

Since no transport current is flowing within the detector gate-gap, two ES are to be in the equilibrium, as depicted in Fig. 1 (b). We therefore can expect the potential of the inner contact in the detector region to be equal to the potential of the outer ES $\mu_{detector} = \mu_{out}$. For the contact combination 1, the detector is situated before the injector, so we can expect $\mu_6^{comb1} = V_1$. For the contact combination 2, the detector is situated after the injector, so $\mu_8^{comb2} = \mu_2^{comb1}$ can be expected.

Our main experimental finding is the fact that both detector potentials $\mu_6^{comb1}, \mu_8^{comb2}$ are significantly smaller than the expected ones: $\mu_6^{comb1} < V_1$ and $\mu_8^{comb2} < \mu_2^{comb1}$, see Fig. 2. The low value of the detector potential indicates that the local equilibrium in the detector region is shifted from the simple relation $\mu_{detector} = \mu_{out}$.

The observed shift $\Delta = \mu_{out} - \mu_{detector}$ is depicted in Fig. 3 (a). It is symmetric at low imbalances $V_1 < V_{th}$, while asymmetry appeares above $V_1 = V_{th}$. For the contact combination 1, $\Delta_1 = V_1 - \mu_6^{comb1}$ monotonically increases with applied imbalance. On the other hand, $\Delta_2 = \mu_2^{comb1} - \mu_8^{comb2}$ changes the slope above $V_1 = V_{th}$.

Electrons are transferred in the injector between two spin-split ES. There are several transfer channels: spin-orbit coupling with emission of non-equilibrium phonon[4]; flip-flop process with DNP creation[6,7,9]; transfer without spin flip to the excited states in the outer ES at high imbalances[8] $V_1 > V_{th}$. Every transfer channel creates each own type of excitations: non-equilibrium phonons, non-equilibrium nuclear spins, and non-equilibrium electrons correspondingly. They are spreading out from the injector region and potentially could shift the local equilibrium in the detector from the expected $\mu_{detector} = \mu_{out}$.

Non-equilibrium phonons are characterized by a distinct distribution direction. In our set-up, they could affect the detector potential only in one contact combination, leaving the other unaffected. This contradicts the experiment, where the shift $\Delta = \mu_{out} - \mu_{detector}$ is symmetric at low imbalances[13], see Fig. 3 (a). Since there is no non-equilibrium electrons at low imbalances $V_1 < V_{th}$, it is the DNP diffusion which is responsible for the low values of the detector potentials.

This conclusion is supported by the hysteresis on the experimental curves, see Fig. 3 (b). The hysteresis on $I - V$ dependencies is a usual demonstration of DNP formation[6,7,9]. The hysteresis reflects a slow relaxation, which originates from establishing the Overhauser field while changing the current.

Let us consider DNP effects in detail. Electron transport in the injector region creates DNP through the flip-flop process[6,7,9]. The DNP area spread out from the injector region because of the nuclear spin diffusion. In the presence of 2DEG, the diffusion can be significantly enhanced through creation of virtual spin excitons[11,12]. In our experimental set-up, spin excitons can exist along the $\nu_c = 1$ incompressible strip only, which makes the diffusion effectively one-dimensional. The corresponding diffusion length can be estimated[12] to be several ten microns. It is consistent with the distance between gate-gap regions in the present experiment. In contrast, the diffusion to the bulk at $\nu = 2$ was found to be very slow[14]

because the cyclotron gap in the bulk suppresses the diffusion through spin exciton.

While existing in the detector region, DNP diminishes the Zeeman splitting between spin-resolved energy levels Δ_c on the Overhauser shift value Δ. In the stationary regime, local equilibrium $\mu_{out} = \mu_{in}$ is established within the detector region, see Fig. 4 (a). We measure chemical potentials of the ES by Ohmic contacts, situated far from the detector region. Leaving the gate-gap, ES also leave the DNP area. The Zeeman splitting is restored to it's value Δ_c, see Fig. 4 (b). The Overhauser shift has no effect on the orbital motion of electrons, so the chemical potential difference Δ appears between spin-resolved ES at the Ohmic contacts. In other words, local equilibrium within DNP region corresponds to the potential difference Δ between spin-resolved ES outside it, as was firstly pointed out in Ref. 15.

The observed Δ is therefore directly the Overhauser shift $\Delta = g\mu_B B_N$ in the detector region of the present structure. The Overhauser field B_N is well known[16] to be significant in 2DEG structures[6,9,15]. In the present experiment, the theoretical limit[16] of the Overhauser field B_N exceeds more than two times the external field B at $\nu = 2$. The relevant g-factor is given by the flat-band condition $eV_{th} = g\mu_B B_{\nu=2}$ in the injector region, so the observed Δ is well below the theoretical limit $eV_{th}B_N/B_{\nu=2}$.

Because virtual spin exciton does not carry an electric charge, DNP diffuse symmetrically to both sides along the 2DEG edge[12]. For this reason, the induced potential shift Δ is independent of the mutual positions of the detector and injector regions at $V_1 < V_{th}$, see Fig. 3 (a).

Symmetry of Δ is broken at high imbalances $V_1 > V_{th}$ because the nuclear spin diffusion becomes asymmetric. Non-equilibrium electrons appear at the empty (excited) energy level in the outer ES in the injector region at $V_1 = V_{th}$, see Fig 1, (c). Their presence partially suppresses the creation of *virtual* spin excitons, and therefore the nuclear spin diffusion, by diminishing the number of empty states at the upper energy level. Because of the magnetic field direction, non-equilibrium electrons exist at one side of the injector region, which makes the nuclear spin diffusion asymmetric.

For the contact combination 1 the right gate-gap is the injector. Due to the magnetic field direction, non-equilibrium electrons are running around all the sample until they could reach the left (detector) gate-gap. In this case non-equilibrium electrons have enough time to relax down in energy, so they do not exist in between the detector and the injector. This justifies the monotonic behavior of Δ at any imbalance for the contact combination 1, see Fig. 3 (a).

For the contact combination 2, the left gate-gap region generates the non-equilibrium electrons. They directly follow in the direction of the detector gate-gap. The nuclear spin diffusion from the injector to the detector is therefore partially suppressed. This is manifested by a slower rise of the Δ at high imbalances in the combination 2, see Fig. 3 (a).

We emphasize, that the asymmetry of the nuclear spin diffusion at high imbalances is a strong confirmation of the one-dimensional diffusion, because the non-equilibrium electrons exist within the $\nu_c = 1$ strip only. We obtain very similar experimental results at $\nu = 4/3, g = 1$ and $\nu = 3, g = 1$ fillings. All these filling factors correspond to the transport through $\nu_c = 1$, i.e. between two spin-split ES like in the $\nu = 2, g = 1$ case.

As a conclusion, we use a novel sample geometry to study non-local effects of edge excitations in the integer quantum Hall effect regime. We find that the condition of local equilibrium at the quantum Hall edge is affected by the diffusion of dynamically polarized nuclei. Our analysis indicates, that the nuclear diffusion is effectively one-dimensional in the present experiment.

We wish to thank V.T. Dolgopolov for fruitful discussions. We gratefully acknowledge financial support by the RFBR, RAS, the Programme "The State Support of Leading Scientific Schools".

---

* Corresponding author. E-mail: dev@issp.ac.ru

1. B. I. Halperin, Phys. Rev. B **25**, 2185 (1982).
2. M. Büttiker, Phys. Rev. B **38**, 9375 (1988).
3. For a review on edge states at low imbalances see R.J. Haug, Semicond. Sci. Technol. **8**, 131 (1993).
4. G. Müller, D. Weiss, A. V. Khaetskii, K. von Klitzing, S. Koch, H. Nickel, W. Schlapp, and R. Lösch, Phys. Rev. B **45**, 3932 (1992).
5. Keith R. Wald, Leo P. Kouwenhoven, Paul L. McEuen, Nijs C. van der Vaart, and C. T. Foxon, Phys. Rev. Lett. 73, 1011 (1994)
6. David C. Dixon, Keith R. Wald, Paul L. McEuen and M. R. Melloch, Phys. Rev. B **56**, 4743 (1997).
7. T. Machida, S. Ishizuka, T. Yamazaki, S. Komiyama, K. Muraki and Y. Hirayama, Phys. Rev. B **65**, 233304 (2002).
8. A. Würtz, R. Wildfeuer, A. Lorke, E. V. Deviatov, and V. T. Dolgopolov, Phys. Rev. B **65**, 075303 (2002); E. V. Deviatov, V. T. Dolgopolov, A. Würtz, JETP Lett. **79**, 618 (2004).
9. E. V. Deviatov, A. Wurtz, A. Lorke, M. Yu. Melnikov, V. T. Dolgopolov, D. Reuter, A. D. Wieck, Phys. Rev. B **69**, 115330 (2004).
10. D. B. Chklovskii, B. I. Shklovskii, and L. I. Glazman, Phys. Rev. B **46**, 4026 (1992).
11. For a review on DNP dynamics see I.D. Vagner, cond-mat/0403087.
12. Yu.A. Bychkov, T. Maniv, and I.D. Vagner, Solid State Comm. **94**, 61 (1995).
13. We should completely rule out possible effects of non-equilibrium phonons. They could potentially shift the local equilibrium by stimulating 'backward' current from the outer ES into the inner one through the spin-orbit coupling. The latter is however characterized by a huge equilibration length[4], which makes the probability of 'backward'

transfer negligible.
[14] T. Nakajima, Y. Kobayashi, S. Komiyama, and M. Tsuboi, accepted in Phys. Rev. B (2010)
[15] A. Würtz, T. Muller, A. Lorke, D. Reuter, and A. D. Wieck, Phys. Rev. Lett. **95**, 056802 (2005)
[16] D. Paget, G. Lampel, B. Sapoval, and V. S. Safarov, Phys. Rev. B **15**, 5780 (1977).